UNIVERSITA' DEGLI STUDI DI PADOVA

Sede Amministrativa: Università degli Studi di Padova

Dipartimento di Scienze Medico-Diagnostiche e Terapie Speciali

DOTTORATO DI RICERCA IN : SCIENZE CARDIOVASCOLARI

CICLO XIX

COMPARATIVE STUDY AT COMPUTED TOMOGRAPHY ANGIOGRAPHY AND INTRAVASCULAR ULTRASOUND OF CORONARY ATHEROSCLEROTIC PLAQUES

Direttore della Scuola : Ch.mo Prof. Gaetano Thiene

Supervisore : Ch.mo Prof. Annalisa Angelini

Dottorando : Giuseppe Maiolino

Summary

Scopo dello Studio. Lo scopo della mia tesi di dottorato e' stato comparare l'accuratezza dell'angiografia coronarica mediante tomografia computerizzata (CTA) a quella dell'ultrasonografia intravascolare (IVUS) nel quantificare placche aterosclerotiche coronariche calcifiche e non. Inoltre, è stata indagata la capacita' della CTA di predire le caratteristiche della placca aterosclerotica determinate all'IVUS ("istologia virtuale", IVUS-VH).

Premessa. La CTA si e' dimostrata affidabile nell'individuare e quantificare le placche coronariche non calcifiche. Le placche calcifiche rappresentano invece tuttora un problema per la sua accuratezza diagnostica, a causa del "partial volume averaging effect", che determina una esagerata rappresentazione nelle immagini delle strutture ad alta attenuazione. L'IVUS-VH utilizza l'analisi spettrale dei dati di radiofrequenza dell'IVUS per costruire mappe tissutali che classificano le placche in quattro componenti maggiori: a) fibrosa, b) fibroadiposa, c) core necrotico e d) calcio. L'IVUS-VH e' uno degli strumenti piu' promettenti sviluppati per la caratterizzazione in vivo delle placche aterosclerotiche e correla bene con l'istologia. La caratterizzazione della placca aterosclerotica alla CTA si e' dimostrata possibile ma problematica. Tuttavia, al momento non vi sono studi che correlino l'analisi della placca aterosclerotica alla CTA e all'IVUS-VH.

Metodi. Sono stati arruolati quarantaquattro pazienti con angina stabile sottoposti a CTA , coronarografia invasiva e IVUS. Sono stati selezionati i segmenti dell'albero coronarico da sottoporre ad indagine CTA dopo comparazione con la coronarografia invasiva e l'IVUS, sulla base di vasi di riferimento individuati con tutte e tre le tecniche. Sono state poi selezionate in cieco, all'oscuro dei risultati della coronarografia invasiva e dell'IVUS, le

immagini della CTA con una workstation dedicata in "multiplanar reformatted reconstructions" in un piano perpendicolare all'asse longitudinale del vaso. Sono state determinate l'area della placca, del lume e del vaso nei segmenti oggetto dello studio ad intervalli di 3 mm. Le placche aterosclerotiche sono state caratterizzate in base ai valori di attenuazione (HU) e le loro componenti classificate come core necrotico (HU 0-29), fibro-adiposa (HU 30–79), fibrosa (HU 80-129) e calcifica (HU ≥130).

Risultati. La CTA e' risultata di qualita' diagnostica in 39 pazienti (42 vasi). E' stata in grado di predire l'area del vaso, del lume, della placca aterosclerotica e la stenosi percentuale del vaso misurati all'IVUS: R^2 0.6 ($p < 0.0001$), 0.5 ($p < 0.0001$), 0.3 ($p < 0.0001$) e 0.2 ($p = 0.04$). Anche dopo aver selezionato per l'analisi solo le sezioni con una componente calcifica nella placca, la CTA e' rimasta capace di predire l'area del vaso, del lume, della placca aterosclerotica e la stenosi percentuale del vaso: R^2 0.5 ($p < 0.0001$), 0.6 ($p < 0.0001$), 0.2 ($p = 0.02$) e 0.2 ($p = 0.04$). Infine, la caratterizzazione della placca aterosclerotica alla CTA si e' dimostrata capace di predire le componenti della stessa derivate all'IVUS-VH: R^2 0.8 core necrotico ($p = 0.02$), 0.5 fibro-adiposa ($p = 0.04$), 0.5 fibrosa ($p = 0.04$) e 0.7 calcifica ($p = 0.02$).

Conclusioni. La CTA e' uno strumento affidabile per la misurazione dell'area del vaso e del lume in presenza di placche coronariche aterosclerotiche calcifiche e non. L'"istologia virtuale" e' fattibile con la CTA e la sua caratterizzazione della placca predice i risultati dell'IVUS-VH.

Aim. The aim of my doctoral thesis was to estimate the accuracy of coronary computed tomography angiography (CTA) in quantifying calcified and non-calcified coronary artery atherosclerotic plaques in comparison with intravascular ultrasound (IVUS). Moreover, the ability of coronary CTA in predicting the IVUS-derived plaque tissue characterization ("virtual histology", IVUS-VH) was assessed.

Background. Coronary CTA proved to be reliable in detecting and quantifying non-calcified coronary plaques. However, calcified plaques are still challenging its diagnostic accuracy, due to the partial volume averaging effect, leading to overrepresentation of high attenuation objects. Intravascular ultrasound-VH uses spectral analysis of IVUS radiofrequency data to construct tissue maps that classify plaques into four major components: a) fibrous, b) fibro-fatty, c) necrotic core, and d) calcium. It is one of the most promising tools developed for *in vivo* plaque tissue characterization and correlates well with histology. Computed tomography plaque characterization demonstrated to be a feasible but challenging task. Currently, there are no published studies comparing coronary CTA plaque analysis with IVUS-VH.

Methods. Forty-four patients with stable angina pectoris who underwent 64-multi-detector CTA, invasive coronary angiography, and IVUS have been enrolled. The coronary tree segments under investigation at coronary CTA after comparison with invasive angiography and IVUS, based on landmark branches detected with all these three techniques have been selected. Coronary CTA images with a dedicated workstation in multiplanar reformatted reconstructions on a plane perpendicular to the vessel longitudinal axis were analyzed, blinded to invasive angiography and IVUS results. For comparison with IVUS, the plaque area, as well as

the lumen and vessel cross sectional area (CSA) at 3 mm intervals in the segments under investigation were investigated. Atherosclerotic plaques were characterized based on CT attenuation values (HU) and their components classified as necrotic core (HU 0-29), fibro-fatty (HU 30–79), fibrous (HU 80-129), and calcified (HU ≥130). .

Results. Coronary CTA was considered of diagnostic quality in 39 patients, 42 vessels. Intravascular ultrasound-determined mean vessel CSA, mean lumen CSA, mean atherosclerotic plaque area and burden were predicted by coronary CTA: R^2 0.6 ($p < 0.0001$), 0.5 ($p < 0.0001$), 0.3 ($p < 0.0001$), and 0.2 ($p = 0.04$), respectively. After selecting the sections with a calcified plaque component, coronary CTA was still able to predict IVUS-derived vessel CSA, mean lumen CSA, mean atherosclerotic plaque area and burden: R^2 0.5 ($p < 0.0001$), 0.6 ($p < 0.0001$), 0.2 ($p = 0.02$), and 0.2 ($p = 0.04$), respectively. Finally, coronary CTA plaque tissue characterization was able to predict IVUS-VH-derived atherosclerotic plaque components: R^2 0.8 for necrotic core ($p = 0.02$), 0.5 for fibro-fatty ($p = 0.04$), 0.5 for fibrous ($p = 0.04$), 0.7 for calcified ($p = 0.02$).

Conclusions. Coronary CTA is a robust tool in measuring vessel and lumen CSA in presence of calcified and non-calcified atherosclerotic coronary plaques. "Virtual histology" is feasible with coronary CTA and its plaque characterization predicts IVUS-VH results.

Background

Computed Tomography

Conventional coronary angiography is an invasive procedure that carries a small but potentially serious risk of major complications, including death, even if performed by an experienced team (1). Moreover, up to 27% of patients who undergo coronary angiography have no significant disease (2-4), thus limiting the benefit from this potentially risky procedure. Therefore, non-invasive assessment of atherosclerotic and non-atherosclerotic coronary artery disease (CAD) is an exciting frontier in cardiovascular medicine that has attracted both invasive and non-invasive cardiovascular specialists, as well as many preventive and public health specialists.

Computed tomography (CT) imaging was first introduced in 1972 and revolutionized medicine with its ability of obtaining cross-sectional images of the body. In 1979 Sir GN Hounsfield and AM Cormack were awarded with the Nobel Prize for medicine for their contribution to the development of this technique.

CT imaging is based on an anode disk that rotates around the patient and emits a fan-shaped beam of x-rays collimated on the slice that will be imaged (5). After the x-rays traveled through the patient their intensity is recorded by detectors positioned at the opposite side. As the person lying on the scanner table is transported through the rotating gantry, a computer reconstructs the cross sectional image based on the x-rays attenuations obtained from multiple angles, using the data generated in a continuous spiral fashion (6). The x-ray attenuation value is expressed in Hounsfield

Units (HU) and each pixel of the reconstructed image is assigned a HU value with a gray-scale image as a final result. The Hounsfield scale is calibrated to give a 0 value for water and -1000 for air. All coronary computed tomography angiography (CTA) post-processing software allows the user to set the window width (the range of HU displayed in an image) and the window level (the HU value at the center of the range). Pixels with a HU number less than the lower limit are displayed as black, HU numbers greater than the upper limit are displayed as white, and the HU number at the center of the range are represented as gray.

Coronary CTA has peculiar challenges to face secondary to cardiac motion and to the small size of the coronary vessels (for a review please refer to (7)). Thus, technical characteristics very important for coronary CTA are temporal and spatial resolution.

The temporal resolution is strictly related to the gantry rotation time, less than 420 ms with the latest generation of scanners. However, the image reconstruction doesn't require a full rotation of the gantry (360 degrees), because of data redundancy. A full cross-sectional image can be reconstructed with data from projections over 180 degrees plus the fan angle (approximately 50 degrees) reducing the actual temporal resolution to half of the gantry rotation time. Despite the continuous technology improvement, the suboptimal temporal resolution is still affecting the quality of the images in coronary CTA, that is strongly related to the heart rate and to the RR interval variability (8-11).

The coronary arteries move at a very high speed: 69 mm/sec for the right, 48 mm/sec for the left circumflex, and 22 mm/sec for the left anterior descending coronary artery (12). Freezing objects moving so fast requires high temporal resolution, otherwise the images will be blurred and non-

interpretable. Lu et al. demonstrated that a minimum scan speed between 35 to 75 ms per slice is needed to completely abolish cardiac motion artifacts (13).

Another important characteristic of coronary CTA is the spatial resolution, i.e. the minimal distance between two features that are still resolved as unique. The most recent scanners have a spatial resolution between 0.75 and 0.5 mm, still inferior to 0.2 mm of invasive coronary angiography (14) and to 0.15-0.25 mm of IVUS (15).

Finally, because the heart is imaged reconstructing multiple slices acquired in a spiral fashion, coronary CTA requires one further prerequisite to provide cross-sectional images without misalignment of the coronary arteries: every displayed image must be at the same heart phase. Therefore, the image reconstruction must be synchronized to a specific phase of the cardiac cycle, using a specific temporal window of the RR interval at the electrocardiogram (ECG) ("retrospective ECG gating") (16).

Coronary Computed Tomography Angiography Validation Studies

The current literature on coronary CTA contains a wealth of data derived mainly from 16- and 64-slice multidetector computed tomography (MDCT) scanners. These scanners are successful in achieving diagnostic images in 93% to 100% of patients, after exclusion of the small diameter vessels (usually <1.5 - 2 mm). Diagnostic yield has continued to improve as CT scanner technology has progressed. The dual-source CT scanner, one of the most advanced CT scanners, is equipped with two 64-slice multidetectors mounted onto the gantry with an angular offset of 90°. It is achieving an unprecedented temporal resolution of 83 ms and it has

showed to offer even better results with a reported diagnostic yield of 100% (17).

Assessment of Native Coronary Arteries

Currently, one of the major coronary CTA indications is the assessment of CAD in symptomatic patients with an intermediate pre-test probability. Specifically, coronary CTA is appropriate for such patients when they have chest pain syndrome and an uninterpretable or equivocal stress test or when they have acute chest pain, but no change in their ECG or cardiac markers (18). Due to its high negative predictive value (NPV), the consensus among most imaging experts is that coronary CTA may be used as a reliable filter before invasive coronary angiography in the assessment of symptomatic patients with intermediate risk of CAD and in patients with uninterpretable or equivocal stress tests (18).

Despite the improved temporal resolution, the latest 64-MDCT technology (gantry rotation speed between 330-400 ms per rotation) it is not capable of freezing the motion of a regular beating heart (i.e. heart rate greater than 70 bpm), so that a small proportion of patients (0-7%) will still have non-diagnostic images, in spite of careful patient selection and of administration of heart rate lowering agents before the scan. The results of the accuracy trials with 64-slice MDCT scanners are encouraging with a per-patient analysis sensitivity of 95-100%, specificity of 83-98%, a positive predictive value (PPV) of 93-97%, and a NPV of 93-100% (19-32). Even more encouraging is the diagnostic accuracy of the dual source CT scanner with a per-patient analysis sensitivity of 95-100%, specificity of 89-98%, a PPV of 74-89%, and a NPV of 99-100% (17, 33, 34). However, the amount of published literature on such a novel technology is still too limited to allow

for any meaningful conclusion on its clinical benefit. Coronary CTA is currently not indicated for asymptomatic patients or for symptomatic patients with a high pre-test probability of having significant CAD (18).

Assessment of Coronary Artery Bypass Grafts

Assessment of the bypass grafts in patients who have had coronary artery bypass grafting (CABG) surgery is often characterized by favorable results with 64-MDCT. Using a per-patient analysis, coronary CTA has demonstrated a good diagnostic accuracy for evaluating graft stenosis with a sensitivity of 100%, a specificity of 71-94%, a PPV of 93-97%, and a NPV of 100% (35-39). However, the assessment of native coronary arteries in post-CABG patients is still limited due to the co-existence of severe native CAD with diffuse and extensive calcified plaques, as well as the often unpredictable beam hardening artifacts from the surgical clips used on the bypass grafts. As a consequence, the percentage of patients post-CABG with disease that cannot be assessed can be as high as 34% (36). Therefore, routine use of coronary CTA for the assessment of symptomatic or asymptomatic post-CABG patients is not indicated. Exceptions are the noninvasive coronary artery mapping, including internal mammary artery, prior to re-op CABG, and selected cases, where useful information on the patency of the bypass grafts and the native runoff vessels could affect the decision-making.

Assessment of Coronary Stents

Clinical utility of coronary CTA in the assessment of stent patency and in-stent restenosis is limited using the current CT scanner technology (18). The major reasons for such limitations are related to inadequate

temporal and spatial resolution. The partial volume effect caused by the metallic stent limits the overall inner lumen visibility. Stent related artifacts are also affected by their diameter and location, as well as the material that it is made out of. In a recently published study, nearly 50% of stents with a diameter ≤3 mm were not interpretable using a 16-slice MDCT scanner (40). Even with the newer 64-slice MDCT technology, as many as 40% of stents cannot be adequately evaluated (41). Stent diameter continues to be an important determinant, with "evaluable" stents having a mean diameter of 3.28 mm compared with a mean diameter of 3.03 mm for "unevaluable" stents (p=0.0002). Despite the disappointingly high rate of unevaluable stents, the NPV and specificity in properly selected cases can still be as high as 99% and 98%, respectively (41, 42).

Intravascular Ultrasound

Invasive coronary angiography is the most established imaging technique used to guide therapy for CAD. Recently, intravascular ultrasound (IVUS) has evolved as a valuable adjunct to angiography. The contributions of IVUS originate principally from two key features, such as its cross-sectional image plan and its ability to directly image the vessel wall. Whereas angiography depicts only a 2-dimensional silhouette of the lumen, IVUS allows precise tomographic measurement of vessel and lumen area, as well as plaque size, distribution, and composition.

Although angiography is still the gold standard used to define coronary anatomy, many studies have challenged its accuracy and reproducibility (43-48). In fact: a) histopathological studies have

demonstrated that angiographic evidence of stenosis is usually not detected until the plaque area approaches 40% to 50% of the total vessel cross-sectional area (CSA) (49-51); b) the visual interpretation of angiograms exhibits significant intra- and inter-observer variability (52); c) any arbitrary angiographic projection can misrepresent the true extent of luminal narrowing, in particular in eccentric stenoses; d) angiography depicts arteries as a planar silhouette of the contrast-filled lumen and doesn't give any information about the vessel wall and the plaque composition, burden, or calcification (50, 53-55); e) the lesion severity assessment requires the lumen diameter measurement within the lesion and an uninvolved "normal" segment, but pathology and IVUS studies demonstrate that disease is usually diffuse, without truly normal segments (55). The tomographic orientation of ultrasound enables a visualization of the full vessel wall, not just two surfaces, and allows an assessment of vessels that are difficult to image by angiography, including diffusely diseased segments, ostial or bifurcation stenoses, eccentric plaques, and angiographically foreshortened vessels.

Intravascular Ultrasound Equipment

The equipment required to perform IVUS consists of two major components, a catheter incorporating a miniaturized transducer and a computer processing the ultrasound signal and reconstructing the image. The ultrasound frequencies used are typically centered at 20 to 50 MHz, providing excellent theoretical resolution. For example, at 30 MHz the wavelength is 50 μm, yielding a practical axial resolution of 150 μm and a lateral resolution, which averages 250 μm at typical coronary artery diameters (15).

The operator advances or retracts the imaging device over the wire either manually or with a motorized pullback at a constant speed (between 0.25 and 1 mm/sec; most frequently 0.5 mm/sec), recording images on videotape or CD for subsequent analysis. Lumen area is determined by planimetry of the leading edge of the blood-intima acoustic interface and affects therapeutic decisions, representing an important application for IVUS. The interface at the border between the media and the adventitia corresponds closely to the location of the external elastic membrane (EEM). The measurement of the area delimitated by the EEM allows the calculation of the plaque area after subtracting the lumen CSA (56).

Comparisons of IVUS lumen area measurements with angiography usually show a close correlation for vessels without atherosclerosis. However, for diseased coronary arteries, investigators report only a moderate correlation ($r = 0.7$ to 0.8) and a standard error >0.5 mm (57-59). The reduced correlation between this two techniques is probably explained by an irregular, noncircular cross-sectional profile, which cannot be adequately depicted by angiography (48).

Intravascular Ultrasound Plaque Characterization and Virtual Histology

Intravascular ultrasound has been used to measure plaque composition on the basis of the ultrasound grayscale tissue reflectance with the aim to identify whether they are prone to rupture or not (60). A stable plaque is characterized by more fibrous tissue or calcification, whereas an unstable plaque has mobile echoes consistent with thrombus or is echolucent because of the necrotic material and large atheroma (60).

However, this tissue characterization doesn't reproducibly discriminate elements of plaque composition (50, 61-64).

Radiofrequency (RF) data analysis from the unprocessed backscattered ultrasound signal, the so-called "virtual histology" (VH), provides an alternative to grayscale image analysis and might provide better information regarding the exact histologic composition of atherosclerotic plaques and possibly their vulnerability to rupture (65). One of the most studied mathematical method applied to RF data analysis includes autoregressive modeling [IVUS-Virtual HistologyTM (IVUS-VH), Volcano Corporation, Rancho Cordova, CA, USA] (66).

Intravascular ultrasound-VH uses spectral analysis of IVUS radiofrequency data to construct tissue maps that classify plaques into four major components: a) fibrous [labeled green], b) fibro-fatty [labeled greenish-yellow], c) necrotic core [labeled red], and d) calcium [labeled white]. These four distinct components of the atherosclerotic plaque may be visualized on histological sections of coronary arteries stained with Movat pentachrome: a) fibrous plaque that comprised of densely packed collagen; b) fibro-fatty plaque consists of collagen and interspersed lipid; c) calcified necrotic plaque that includes cholesterol clefts, foam cells, and micro-calcifications; and d) calcified plaque without adjacent necrosis (66).

In explanted human atherosclerotic arteries IVUS-VH tissue maps identifies the four plaque types when compared with the corresponding histological sections with a sensitivity, specificity, and predictive accuracy of 80–92% (66). Moreover, IVUS-VH coronary plaques characterization generated by *in vivo* pullbacks have been compared with histological sections obtained from directional coronary atherectomy (DCA) (67) and identified plaque components with a predictive accuracy of 87% for fibrous,

87% for fibro-fatty, 88% for necrotic core, and 97% for dense calcium regions. However, Granada et al. (68) recently questioned the accuracy of IVUS-VH in assessing plaque composition in an atherosclerotic porcine model. In fact, when compared with histology, IVUS-VH identified plaque components with a disappointing low accuracy of 38–58%.

Noteworthy, the current literature on the IVUS-VH have significant methodological limitations and therefore more studies are required to validate this technique from the clinical standpoint (69). The construction and validation of tissue maps for IVUS-VH identified plaque components by Movat pentachrome stain. Given the complexity of the atherosclerotic plaque these tissue stains are subject to variable interpretation. Moreover, a histological section and an IVUS-VH frame image different plaque thickness along the longitudinal axis of the vessel. In fact, a histological section may be as thin as 4 μm, whereas IVUS-VH data derives from an ultrasound beam whose width may be as great as 300 μm at its interface with the arterial wall. As a consequence, IVUS-VH is unlikely to detect subtle changes in plaque composition that occur over small distances (70).

Intravascular Ultrasound and Coronary Computed Tomography Contribute in Detecting Plaque Features Predictive of Acute Events

Acute coronary syndromes (ACS) are precipitated by the development of an intraluminal coronary thrombus. Insights into the pathology precursors of plaque rupture and subsequent coronary thrombosis have predominantly arisen from necropsy studies in patients who experienced sudden cardiac death (71, 72). Coronary thrombosis is associated with three plaque characteristics: plaque rupture, plaque erosion, and calcified nodules (73). Plaque rupture occurs in a majority of

lesions that have overlying thrombi and its histological precursor has been designated as the thin cap fibroatheroma (TCFA), defined as a lesion with a fibrous cap 65 μm thick, infiltrated with macrophages, with a well developed necrotic core (73).

Another important contribute to detection of vulnerable plaques originates from IVUS, with *in vivo* studies in ACS patients. The expansive arterial remodeling, defined as an enlargement of the EEM CSA in the presence of atheroma, namely the Glagov phenomenon (49), was demonstrated to occur more often in the culprit lesions (74, 75). Moreover, the presence of small coronary calcium deposits is more frequent in the culprit lesions of ACS compared to atherosclerotic plaques of stable angina pectoris patients (76).

One of the most relevant research fields in the modern cardiology era is the detection of plaques at risk of rupture, allowing a preventive medical or interventional therapeutic action to avoid acute catastrophic events. Intravascular ultrasound-VH is one of the most promising tools developed with this aim. Provided its close association with coronary thrombosis, a surrogate for histological TCFA will be a relevant information to define the patient risk of future events. Rodriguez-Granillo et al. performed an analysis to detect TCFA with IVUS-VH in 55 patients (77). IVUS-derived TCFA was defined as the presence of a focal, necrotic-core rich (>10%) plaque in contact with the lumen, with a percent atheroma CSA >40%. The investigators determined that IVUS-derived TCFA was more prevalent in ACS patients and occurred more commonly in the proximal segments of arteries. A potential limitation of this study is the axial resolution and spatial accuracy of IVUS-VH. Intravascular ultrasound-VH has an axial resolution of 150 μm and a spatial accuracy of 240 μm (66),

whereas the accepted histological definition for TCFA requires a thinner fibrous cap (73). Moreover, IVUS-VH cannot visualize cellular components such as T cells and macrophages, both crucial features of histological TCFA. Clearly, IVUS-derived TCFA is an entity distinct from histological TCFA, and its importance will need to be assessed in longitudinal studies.

As previously mentioned, another characteristic of unstable plaques is the positive remodeling. Grayscale IVUS studies have shown that culprit lesions in ACS occur more often in areas of expansive remodeling (74). Therefore, investigators have used IVUS-VH to assess plaque composition in areas of expansive remodeling (78, 79). Lesions with expansive remodeling had a larger necrotic core and less fibrous tissue when compared with non-remodeled lesions or lesions with constrictive remodeling (decrease in the EEM CSA). Lesions with expansive remodeling were predominantly composed of fibro-fatty tissue (fibroatheromatous) or IVUS-derived TCFA. In contrast, only a small number of lesions with constrictive remodeling were fibroatheromatous and none had IVUS-derived TCFA (78). These cross-sectional studies suggest that atherosclerotic lesions with expansive remodeling have different plaque composition than lesions with constrictive remodeling. It remains unknown whether these compositional differences are predictive of thrombotic events.

Autopsy studies suggest that the majority of occlusive intracoronary thrombotic events arise from plaque rupture. Therefore, assessment of ruptured plaque may provide insight into the features of vulnerable plaque. Recently, Rodriguez-Granillo et al. (80) described IVUS-VH-derived plaque composition in lesions with plaque rupture. Forty patients with ACS underwent three-vessel IVUS. Plaque rupture occurred in 28 lesions (20

patients). Disrupted lesions compared with those without plaque rupture had similar plaque burden but a larger EEM CSA, findings indicative of greater expansive remodeling in ruptured lesions. Ruptured plaque also had a greater percentage of necrotic core. This study is consistent with earlier reports that linked expansive remodeling with coronary events and reveals a correlation between IVUS-VH-detected necrotic core and plaque rupture.

Noteworthy, in a recent study Motoyama et al. (81) were able to demonstrate that 400/16 x 0.5-MDCT and 350/64 x 0.5-MDCT are a useful tool in detecting plaque vulnerability features. This group enrolled 38 patients with ACS and compared their plaque characteristics with those of 33 patients with stable angina pectoris. Positive remodeling (87% vs. 12%, $p < 0.0001$), non calcified plaque density <30 HU (79% vs. 9%, $p < 0.0001$), and spotty calcification (63% vs. 21%, $p = 0.0005$) were significantly more frequent in the culprit ACS lesions than in plaques of patients with stable angina pectoris. Moreover, no acute event occurred when the plaque didn't have any of the three high-risk features (i.e., positive remodeling, non calcified plaque density <30 HU, or spotty calcification).

The aim of plaque tissue characterization is to improve the detection of those at high risk of rupture, which itself is a controversial concept. Although histological examination of coronary arteries from victims of sudden cardiac death have shown that TCFA is commonly associated with plaque rupture, the significance of TCFA in living subjects is still unknown. Moreover, evidence of multiple disrupted plaques and widespread inflammation throughout the vascular bed in some patients with ACS (82, 83), suggests that it may be more appropriate to focus attention at a

systemic level, i.e. towards the vulnerable patient. Only the results of large, prospective studies with long-term follow-up will determine whether the identification of vulnerable plaque by means of any modality is diagnostically and therapeutically useful (69).

Multidetector Computed Tomography and Intravascular Ultrasound Comparative Studies

Despite invasive coronary angiography is currently the imaging tool used to guide therapy for CAD, one of the most interesting points recently raised is that it may not represent the gold standard to determine the diagnostic accuracy of coronary CTA. In fact, it can be misleading to compare a technique detecting disease severity based on a two-dimensional assessment, the minimal lumen diameter at invasive angiography, with coronary CTA, that allows a three-dimensional view of the vessel.

Two recent reports strengthen this view. Caussin at al. (84) demonstrated with a 330/64 x 0.4-MDCT that in 36 patients with intermediate *de novo* lesions (between 30% to 70% of luminal narrowing at invasive angiography) the minimal lumen area at coronary CTA has a good correlation with IVUS ($r = 0.88$, $p < 0.001$). Noteworthy, using IVUS as a gold standard, the classification of these stenosis as hemodynamically significant or not is better accomplished with coronary CTA (sensitivity and specificity of 87% and 72%, respectively) than with invasive angiography (sensitivity and specificity of 24% and 56%, respectively). This finding was recently confirmed by a study limited to left main coronary artery borderline stenosis comparing 420/16 x 0.75-MDCT to invasive

angiography and IVUS (85). Whereas there was a good correlation between IVUS and coronary CTA for minimal lumen diameter ($r = 0.77$, $p < 0.01$), there was only a moderate correlation between invasive angiography and IVUS ($r = 0.52$, $p < 0.05$).

Multiple reports confirm the good diagnostic performance of coronary CTA compared to IVUS. In an *in vivo* human study, diagnostic accuracy of 420/12 x 0.75-MDCT was high, with a sensitivity of 91% and a specificity of 97% in identifying atherosclerotic plaques detected by IVUS (86). These results were recently confirmed by another group with 420/16 x 0.75-MDCT with a sensitivity, specificity, PPV and NPV of 86%, 69%, 90%, and 61%, respectively, for detection plaques classified as significant (>50% of vessel CSA obstruction) (87). In a more recent study with the same generation of scanners Iriart et al. (88) demonstrated a good diagnostic accuracy of 420/16 x 0.75-MDCT compared to IVUS in detecting coronary plaques, with a sensitivity, specificity, PPV, and NPV of 79%, 99%, 99%, and 82%, respectively. The authors also confirmed a good correlation between the two techniques in measuring the minimal lumen area and the vessel CSA ($r = 0.81$ and 0.70, respectively; $p < 0.001$).

Two more detailed studies comparing 420/12 x 0.75-MDCT with IVUS, also showed high sensitivities (94% to 95%) and specificities (92% to 94%) for detection of calcified plaques (89, 90). However, these rewarding results were strongly dependent on the presence of partial or complete calcification of the lesion analyzed. In fact, the sensitivity for detection of exclusively noncalcified plaques dropped to 53% (89) and 78% (90).

Leber et al. (20) completed one of the first study of comparison between coronary CTA and IVUS with the latest generation of scanners. They analyzed by 330/64 x 0.6-MDCT 59 patients originally scheduled for

conventional angiography because of stable angina pectoris and performed IVUS in 32 coronary arteries with <50% luminal stenoses at invasive angiography. Overall sensitivity and specificity to detect nonsignificant coronary plaques by coronary CTA were 84% and 91%, respectively. However, despite using state of the art technology, namely the 330/32 x 0.6-MDCT, the same group (91) demonstrated that detection of exclusively non-calcified lesions is still a challenge with a sensitivity of 83% compared to IVUS. Moreover, non-calcified and mixed plaque volumes were systematically underestimated by coronary CTA compared to IVUS (59.8 ± 76.6 mm^3 vs. 67.7 ± 67.9 mm^3 and 47.7 ± 87.5 mm^3 vs. 57.5 ± 99.4 mm^3, respectively, p <0.03), whereas calcified plaque volumes were overestimated (65.8 ± 110.0 mm^3 vs. 53.2 ± 90.3 mm^3, p = NS).

A further confirm to coronary CTA diagnostic accuracy originates from a study completed by Leber et al. (20) comparing 330/64 x 0.6-MDCT and IVUS. The authors demonstrated a good agreement and correlation between coronary CTA and IVUS for the measurement of vessel and lumen CSA: 8.4 ± 4.5 mm^2 vs. 9.4 ± 5.1 mm^2 (p <0.01), 16.4 ± 5.8 mm^2 vs. 16.7 ± 7.1 mm^2 (p = 0.6, NS), r = 0.81 and 0.88, respectively.

One of the more exciting and promising field in cardiology research is the detection of patients or plaques at risk for future events, namely vulnerable patients or plaques. A relevant effort is ongoing in multiple top investigative centers to image invasively and non- atherosclerotic lesions prone to rupture. An increasing wealth of studies is conducted in an attempt to relate specific CT densities with different atherosclerotic plaque components and these efforts are becoming more rewarding as the technology improves.

Initial reports in patients showed that even 500/4 x 1.0-MDCT could achieve some differentiation between non-calcified and calcified plaques both *in vivo* (92, 93) and *ex vivo* (94), with findings confirmed by IVUS in the former and by histopathology in the latter. The German group was able to demonstrate in two small series that overall CT densities steadily increased as coronary plaques were classified as soft, intermediate, and calcified, based on IVUS criteria (92, 93). More recently, Iriart et al. (88) confirmed that plaque tissue characterization with 420/16 x 0.75-MDCT is feasible. Plaques defined as hypoechoic, hyperechoic, and calcified at IVUS have different density features at coronary CTA, 38 HU, 94 HU, 561 HU, respectively ($p < 0.001$).

Schoenhagen et al. (95) demonstrated that discrimination between calcified and noncalcified plaques was high, with a diagnostic accuracy of 0.88-0.93, and a good interobserver agreement. These results were subsequently confirmed by Komatsu et al. (96) who enrolled 45 patients with ACS and compared plaque characterization by 500/8 x 1.25-MDCT and IVUS. They demonstrated sensitivities of 92%, 87%, and 89% for detection of soft, intermediate, and calcified plaques, respectively. However, these exciting results are partially mitigated by another study (97) demonstrating that 420/16 x 0.75-MDCT is able to discriminate hypoechoic from hyperechoic plaques (58 ± 43 HU and 121 ± 34 HU, respectively; $p < 0.001$), but there is a significant overlap of the measured CT attenuations.

Being able to image the contrast filled lumen and the vessel wall coronary CTA is very appealing for the measurement of the atherosclerotic plaque area and volume, as well as to estimate the atherosclerotic burden. Unfortunately, the technology is still facing major challenges secondary to a

suboptimal spatial resolution and, as a consequence, the measurements are still lacking consistency and reproducibility.

Achenbach et al. (89) demonstrated that despite a relatively good correlation ($r = 0.8$, $p < 0.001$) between 420/12 x 0.75-MDCT and IVUS, the former systematically underestimates plaque volume. Overall mean plaque volume per segment by 420/12 x 0.75-MDCT was 24 ± 35 mm^3, whereas by IVUS it was 43 ± 60 mm^3 ($p < 0.001$). In a more recent study the same group demonstrated that in 26 patients the plaque area tended to be overestimated by 420/16 x 0.75-MDCT in comparison to IVUS (86). In this latter study, the mean cross-sectional plaque area was 8.3 ± 4.8 mm^2 by coronary CTA and 7.3 ± 3.1 mm^2 by IVUS, showing only a moderate correlation ($r = 0.55$, $p < 0.001$). Such conflicting results coming from the same group could be partially explained by the relatively small number of patients enrolled and by use of different methodologies.

Another study limited to left main coronary artery borderline stenosis compared 420/16 x 0.75-MDCT and IVUS (85). Minimal lumen diameter was slightly underestimated (0.3 ± 0.5 mm), as well as lumen area stenosis ($3.7 \pm 10.1\%$), and plaque burden ($0.4 \pm 6.7\%$), whereas minimal lumen area was overestimated (0.2 ± 1.5 mm^2) by coronary CTA. Leber et al. (20) analyzed 59 patients with the latest CT technology available and found that mean plaque areas as determined by 330/64 x 0.6-MDCT and IVUS were 7.3 ± 5.1 mm^2 and 8.1 ± 3.8 mm^2, respectively ($p < 0.04$), with a correlation coefficient for these measurements of 0.73.

As previously highlighted, one of the plaque vulnerability features is considered the vessel positive remodeling (75, 98). *In vivo* plaque remodeling assessment in humans by MDCT is feasible with consistent results.

In a study involving 44 patients showing atherosclerotic plaques only in proximal coronary artery segments, Achenbach et al. (99) were able to compare 420/12 x 0.75-MDCT with IVUS-derived vessel CSA in 13 individuals (26 sites, mean MDCT: 20 ± 7 mm^2, mean IVUS: 18 ± 8 mm^2). The Bland-Altman analysis showed a bias toward larger vessel areas with coronary CTA (mean difference: 1.2 mm^2). The remodeling index was 1.1 ± 0.3 at coronary CTA and 1.1 ± 0.4 at IVUS (r^2 = 0.82, p = 0.001). The feasibility in detecting the remodeling index was also recently confirmed by Kitagawa et al. (100) with a good correlation between IVUS and 350/64 x 0.625-MDCT (r = 0.88, p <0.001). These authors were also able to prove the reliability of coronary CTA in detecting another feature of plaque vulnerability, namely the spotty calcification, correctly detected in 12 of 14 plaques. Finally, while studying by 420/16 x 0.75-MDCT 22 patients presenting with ACS, Caussin et al. (101) showed a good diagnostic accuracy of coronary CTA for detection of IVUS-derived vulnerability features, like positive remodeling and echolucency (100%, 81%, and 90%, 80% sensitivity and specificity, respectively).

Methods

Patients

From October 2005 to July 2006, we enrolled 44 patients without previously known CAD who underwent coronary CTA, invasive coronary angiography, and IVUS because of angina pectoris. Exclusion criteria were: impaired renal function (plasma creatinine >1.5 mg/dL), unstable clinical condition, known allergy to iodinated contrast media, pregnancy, and severe obesity (body mass index >35). The coronary CTA was performed within four days before coronary angiography in all patients. The study protocol was approved by the institutional ethics committee of the Cabrini Medical Center, Mount Sinai School of Medicine, and Columbia University and all patients gave informed consent to participate in the study.

Computed Tomography Angiography.

All examinations were performed with a 64-slice MDCT scanner (Somatom Sensation 64, Siemens, Forchheim, Germany; Toshiba Multi-Slice Aquilion 64,Toshiba Medical Systems, Tokyo, Japan). Before the examination, an intravenous line (18-20 gauge) was placed in the antecubital vein and the patient was connected to the ECG monitor. Five to 20 mg of metoprolol were given intravenously immediately before the scan if the heart rate was >65 bpm. Contraindications for beta blockade included atrioventricular block (second degree or greater), severe left ventricular systolic dysfunction (ejection fraction <35%), or cardiac disease with potential for decompensation (such as severe aortic stenosis). If there was a history of allergy to beta-blockers or bronchial hyperreactivity, intravenous diltiazem was used as an alternative. Immediately before the scan the patients received 0.4 mg of sublingual nitroglycerin to obtain vasodilatation of the coronary tree.

A test bolus of 20 ml of contrast was injected and a single axial plane at the level of the aortic root was acquired with a region of interest placed in the ascending aorta in order to monitor contrast arrival. The scanning delay was then determined as the interval from the start of injection to peak enhancement in the ascending aorta, plus 3 seconds. Subsequently, a continuous infusion of 60-80 mL of iodinated contrast agent was initiated at a rate of 4-5 mL/sec followed by a 50-ml saline chaser. The images were acquired with these parameters: 32 x 0.6 mm collimation with dual focal spots per detector row, rotation time 330 ms, table feed 3.8 mm/rotation, tube voltage 120 kV, effective mA 750 to 900 for the Siemens MDCT; 64 x 0.5 mm collimation, a rotation time of 400 ms, and a tube current of 300 mA at 120 kV for the Toshiba MDCT. Current modulation was used reducing the tube current during the systolic phase of the cardiac cycle, in order to decrease the radiation exposure during this phase to 20%.

Computed Tomography Angiography Images Reconstruction Protocol

Cross-sectional images (0.6-0.5 mm thickness, 0.4-mm overlap) were reconstructed using retrospective ECG gating. A dedicated half-scan algorithm was used, leading to an acquisition time of 165-200 ms (the multisegment reconstruction option was disabled). Multiple reconstructions were performed per patient at 40% to 70% of the RR interval and the best reconstructions for image quality were transferred to a dedicated workstation (Aquarius, Terarecon Inc, San Mateo, CA) and used for analysis. The 2D axial images and 3D postprocessing tools (multiplanar reformatted imaging, maximum intensity projection, and volume rendering) were subsequently employed for analysis.

Computed Tomography Angiography Images Analysis

An investigator selected the coronary tree segments under investigation at coronary CTA after comparison with invasive angiography and IVUS, based on landmark branches detected with all these three techniques. Another experienced reader, blinded to invasive angiography and IVUS results, analyzed the coronary CTA images with a dedicated workstation (Aquarius Workstation, Terarecon inc, San Mateo, California).

On a first analysis, the image quality was determined based on the presence of motion artifacts and contrast-to-noise ratio. Motion artifacts were defined as blurring of the artery borders, "step" artifacts, or vessel duplication. The studies were graded for image quality, based on the presence of motion artifacts in the main coronary arteries under investigation using a 3 point score (1: no artifact, 2: mild artifact that doesn't affect evaluation of segments, 3: non-evaluable segment). Only coronary arteries devoid of artifacts were included in the analysis.

The contrast-to-noise ratio was calculated in all the scans, using a region of interest in the ascending aorta, as the ratio between the mean HU in the region of interest and its standard deviation (102). A high-quality image was defined if the contrast-to-noise ratio was >8; a moderate-quality image was defined by a contrast-to-noise ratio between 4 and 8; and a poor-quality image was defined by a contrast-to-noise ratio <4. Only patients who had high or moderate quality images were considered for further analysis.

Any structure with a density of 130 HU or more was defined as calcified atherosclerotic plaque if it: 1) could be visualized separately from the contrast-enhanced coronary lumen (either because it was "embedded"

within non-calcified plaque or because its density was above the contrast-enhanced lumen); 2) could be assigned to the coronary artery wall; and 3) could be identified in at least two independent planes. Structures clearly assignable to the vessel wall (in at least two views) with densities less than the lumen contrast were classified as non-calcified plaque components. Every plaque was analyzed based on its CT attenuation value and classified as necrotic core (HU 0-29), fibro-fatty (HU 30–79), fibrous (HU 80-129), and calcified (HU ≥130) based on previous reports (103, 104) and on our laboratory unpublished results.

The display setting used for lumen and plaque quantification was determined empirically in a subset of seven patients. In each patient, at multiple coronary sites 3 mm apart, vessel and lumen CSA were calculated with different window width and window level settings. At this analysis, the optimal settings to detect plaque and outer vessel boundaries were a window width representing 155% and a window level representing 80% of the mean attenuation value within the lumen. However, when calcified plaques not embedded within a non-calcified plaque were present a different setting was necessary, to account for the calcium partial volume averaging effect. In these circumstances, the window width was set at 900 HU and the window level at 350 HU. Keeping the window level (80% of mean intensity within the corresponding lumen) and reducing the width to a HU value of one, provided optimal matching with IVUS lumen CSA. For comparison with IVUS, using multiplanar reformatted imaging in the cross sections of the coronary arteries, we determined the plaque area, as well as the lumen and vessel CSA at 3 mm intervals in the segments under investigation.

Intravascular Ultrasound

The IVUS was performed as part of the invasive diagnostic procedure (motorized pullback at 0.5 mm/sec, electronic 20-MHz Volcano Eagle EyeTM transducer, Volcano Therapeutics, Rancho Cordova, California) in 47 coronary arteries without significant coronary stenoses (<50%) at invasive angiography. The EEM CSA, the lumen CSA, and the plaque area, defined as lumen CSA subtracted from EEM CSA, was calculated in the segments under investigation every 3 mm. The measurements were performed in accordance to the IVUS interpretation guidelines of the American College of Cardiology and the American Heart Association (56). Moreover, the atherosclerotic coronary plaques underwent tissue characterization based on mathematical autoregressive spectral analysis of IVUS backscattered data (IVUSLab software, Volcano Therapeutics, Rancho Cordova, California). On the reconstructed color-coded tissue map fibrous areas were labeled in green, fibro-fatty in greenish-yellow, necrotic core in red, and calcium in white. The absolute area of each plaque component in the tissue map was calculated automatically by IVUSLab software.

Comparison of 64-slice CT and IVUS

To ensure that the same corresponding coronary sections were compared at IVUS and MDCT, a reader selected reference points detectable with both techniques and identified the coronary segments using a 17-segment modified AHA classification (19, 105).

Starting from the distal reference point, the coronary vessel was analyzed in 3-mm intervals and each section was directly compared with both methods regarding a) the plaque burden (plaque plus media CSA

divided by EEM CSA), b) the EEM CSA, and c) the lumen area. Finally, we calculated for every section the plaque composition (necrotic core, fibro-fatty, fibrous, and calcified).

Statistical Analysis.

All variables were formally tested for Gaussian distribution by Kolmogorov-Smirnov test. Vessel and lumen CSA, plaque area and burden determined at IVUS and coronary CTA were compared using Bland-Altman analysis. The ability of coronary CTA to predict the vessel and lumen CSA, plaque area and burden, and plaque composition detected at IVUS was determined at linear regression analysis.

Statistical significance was defined as $p < 0.05$. SPSS 13.0 for Windows (SPSS Italy Inc., Bologna, Italy) was used for all analyses.

Results

According to the inclusion criteria, coronary CTA was performed successfully and without any complication in 44 patients (age 55 ± 13 years) who subsequently underwent invasive coronary angiography and IVUS (47 vessels). Beta-blockers to reduce the heart rate were given to all patients during coronary CTA. The mean heart rate during the scan was 60 ± 9 beats/min. Five out of 44 patients had coronary CTA that was affected by motion artifacts (n = 4) in the segment studied by IVUS or poor contrast-to-noise ratio (n = 1), making the evaluation of the coronary segments under investigation not possible. Diagnostic coronary CTA image quality was obtained in 39 patients and 42 vessels. A total of 336 sections at coronary CTA were available for the comparison with IVUS.

Bland-Altman analysis showed that mean vessel and lumen CSA were systematically overestimated by coronary CTA (16.0 ± 6.4 mm^2 vs. 17.6 ± 7.7 mm^2 and 8.6 ± 3.5 mm^2 vs. 10.4 ± 4.3 mm^2, IVUS and coronary CTA, respectively, $p < 0.01$). The Bland-Altman plots and the correlation diagrams for determination of mean vessel and lumen CSA are given in Figures 1 and 2. At linear regression analysis coronary CTA was able to predict IVUS measurements: adjusted R^2 being 0.6 for mean vessel CSA ($p < 0.0001$) and 0.5 for mean lumen CSA ($p < 0.0001$).

Moreover, Bland-Altman analysis showed that mean plaque area and burden were systematically underestimated by coronary CTA (7.4 ± 4.0 mm^2 vs. 7.3 ± 5.5 mm^2 and 0.4 ± 0.2 vs. 0.4 ± 0.1 mm^2, IVUS and coronary CTA, respectively, $p < 0.01$). The Bland-Altman plots and the correlation diagrams for determination of mean plaque CSA and burden are given in Figures 3 and 4. At linear regression analysis coronary CTA was able to predict IVUS measurements: adjusted R^2 being 0.3 for mean plaque CSA measurement ($p < 0.0001$) and 0.2 for plaque burden measurement ($p = 0.04$).

To assess the reliability of the window width and window level setting used to analyze the calcified plaques, we repeated the analysis in the subgroup of sections found to have a calcified plaque component at IVUS (n = 145). Bland-Altman analysis showed that mean vessel and lumen CSA were again systematically overestimated by coronary CTA (18.5 ± 7.1 mm^2 vs. 21.6 ± 7.7 mm^2 and 8.8 ± 4.5 mm^2 vs. 12.4 ± 4.4 mm^2, IVUS and coronary CTA, respectively, $p < 0.01$). At linear regression analysis coronary CTA was able to predict IVUS measurements with an adjusted R^2 of 0.5 for mean vessel CSA ($p < 0.0001$) and of 0.6 for mean lumen CSA ($p < 0.0001$). Again, Bland-Altman analysis showed that mean plaque area and burden were systematically underestimated by coronary CTA (9.7 ± 3.7 mm^2 vs. 9.2 ± 6.1 mm^2 and 0.5 ± 0.1 vs. 0.4 ± 0.2 mm^2, IVUS and coronary CTA, respectively, $p < 0.01$). At linear regression analysis, coronary CTA was still able to predict IVUS mean plaque CSA measurement (adjusted R^2 0.2, $p = 0.02$) and plaque burden measurement (adjusted R^2 0.2, $p = 0.04$).

In a subset of 24 patients, 25 vessels, we were able to compare the IVUS-VH-derived plaque characteristics with coronary CTA. A representative example of IVUS and coronary CTA plaque characterization is given in Figures 5-7. The plaque IVUS-VH-subsets and coronary CTA were 5.2 ± 3.9 mm^2 vs. 11.9 ± 5.1 mm^2 for necrotic core, 18.5 ± 13.6 mm^2 vs. 11.9 ± 6.3 mm^2 for fibro-fatty, 48.2 ± 32.7 mm^2 vs. 18.4 ± 8.8 mm^2 for fibrous, 2.3 ± 1.7 mm^2 vs. 29.8 ± 14.7 mm^2 for calcified, respectively. At linear regression analysis, coronary CTA demonstrated to predict well the atherosclerotic plaques tissue characteristics when compared to IVUS-VH. In fact, the adjusted R^2 for the plaque features were: 0.8 for necrotic core ($p = 0.02$), 0.5 for fibro-fatty ($p < 0.05$), 0.5 for fibrous ($p < 0.05$), and 0.7 for calcified ($p = 0.02$).

Discussion

Our study demonstrated that, in comparison with IVUS, coronary CTA a) is capable to measure and predict with good accuracy the vessel and lumen CSA, b) is moderately accurate in determining the mean plaque area and burden, c) is able to reliably measure vessel and lumen CSA, mean plaque area and burden in presence of calcified plaques, and d) is capable to predict the plaque tissue characteristics derived at IVUS-VH.

Coronary Computed Tomography Angiography Reliability in Measuring Plaque Burden, Vessel and Lumen Area

Multiple studies confirm the good diagnostic performance of coronary CTA compared with IVUS. Sixteen- and 64-MDCT diagnostic accuracy was high with a sensitivity, specificity, PPV, and NPV for detecting atherosclerotic plaques of 79-95%, 86-99%, 91-99%, and 76-82%, respectively (20, 86, 88-90) and of 86%, 69%, 90%, and 61%, respectively, for detection of plaques classified as significant (>50% of vessel CSA obstruction) (87). Moreover, at least for the analysis of intermediate lesions (between 30% to 70% of luminal diameter stenosis at invasive angiography), coronary CTA, with a sensitivity and specificity of 87% and 72%, respectively, compares favorably to invasive coronary angiography (sensitivity and specificity of 24% and 56%, respectively) (84).

Despite the spatial resolution is less than half compared to invasive angiography (0.5-0.75 mm and 0.2 mm, respectively (14)), coronary CTA has a great advantage over the latter. It's able to image the contrast filled lumen and the coronary vessel wall, and it's not mere "luminography" as invasive angiography (48). Unfortunately, the measurements derived from coronary CTA are still lacking consistency and reproducibility, partially because the published literature is lacking strict criteria of image analysis,

for example in windowing parameters, with a noteworthy exception coming from Dr. Becker's group (20, 91).

Therefore, we tried to use a consistent method in deriving our measurements with predefined image windowing at coronary CTA, as suggested by a Funabashi's et al. study (106) and as already performed by Leber et al. (20). We found that coronary CTA systematically overestimated the mean vessel and lumen CSA (16.0 ± 6.4 mm^2 vs. 17.6 ± 7.7 mm^2 and 8.6 ± 3.5 mm^2 vs. 10.4 ± 4.3 mm^2, IVUS and coronary CTA, respectively, $p < 0.01$) and underestimated the mean plaque area and burden (7.4 ± 4.0 mm^2 vs. 7.3 ± 5.5 mm^2 and 0.4 ± 0.2 vs. 0.4 ± 0.1 mm^2, IVUS and coronary CTA, respectively, $p < 0.01$). Moreover, we were able to demonstrate that coronary CTA is able to predict with good accuracy mean vessel and lumen CSA determined at IVUS (adjusted R^2 of 0.6 ($p < 0.0001$) and 0.5 ($p < 0.0001$), respectively), whereas has only low accuracy in predicting the mean plaque area and burden (adjusted R^2 of 0.3 ($p < 0.0001$) and 0.2 ($p = 0.04$), respectively).

Our data confirm a previous study by Leber et al. (20) comparing 330/64 x 0.6-MDCT with IVUS, that was performed with similar methodology. The authors demonstrated a good agreement between coronary CTA and IVUS for the measurement of vessel and lumen CSA, with a tendency toward overestimation of the former technique compared to the latter: 16.7 ± 7.1 mm^2 vs. 16.4 ± 5.8 mm^2 ($p = 0.6$, NS) and 9.4 ± 5.1 mm^2 vs. 8.4 ± 4.5 mm^2 ($p < 0.01$), respectively. Moreover, there was a good correlation between the two diagnostic tools for both measurements: $r = 0.81$ and 0.88, respectively.

Our study is also consistent with the results of a previous paper by Achenbach et al. (89) demonstrating that 420/12 x 0.75-MDCT

systematically underestimates plaque volume compared to IVUS (24 ± 35 mm^3 vs. 43 ± 60 mm^3, respectively; p <0.001). However, in a more recent study the same group demonstrated in 26 patients that plaque area tended to be overestimated by 420/16 x 0.75-MDCT in comparison to IVUS: 8.3 ± 4.8 mm^2 vs. 7.3 ± 3.1 mm^2, respectively, with a moderate correlation; r = 0.55, p <0.001) (86). A study carried out with the latest MDCT technology available (20), the same of our scanners, demonstrated again that coronary CTA underestimate the mean plaque area compared to IVUS (7.3 ± 5.1 mm^2 vs. 8.1 ± 3.8 mm^2, respectively; p <0.04), with a correlation coefficient for these measurements of 0.73. Dragu et al. (85), in a study limited to left main coronary artery borderline stenosis, found that the plaque burden was overestimated by 420/16 x 0.75-MDCT compared to IVUS (49.2 ± 19.7% vs. 49.2 ± 15.8%), with a very high correlation (r = 0.94; p <0.01).

Such conflicting results, among our work and some of the published studies, are probably secondary to the use of different coronary CTA images reading settings and highlights again the lack of consistency and reproducibility of these measurements when different windowing parameters are used. Moreover, when we tried to use imaging settings already published in literature (20), our coronary CTA results were not consistent with IVUS. This could be probably attributed to different patients cohorts and plaque characteristics, as well as to differences in the scanner and in the software used.

In conclusion, our results on coronary CTA-IVUS comparison in the measurement of the mean vessel and lumen CSA, mean plaque area and burden are in agreement with the studies published to date with methodology similar to ours. Our statistic approach was different from most of the current literature because our aim was not to demonstrate an

association between the two tools, but to determine at linear regression analysis if coronary CTA was able to predict IVUS measurements.

Coronary Computed Tomography Angiography Reliability in Measurements Derived in Presence of Calcified Plaques

One of the major coronary CTA problems is the overestimation of the calcified plaques, secondary to the so-called partial volume averaging. The HU number assigned to each pixel is proportional to the average attenuation coefficient (μ) in the corresponding voxel. For voxels containing one tissue type, μ is representative of that tissue. However, some voxels in the image contain a mixture of different tissue types. In this case, the μ is not representative of either tissue, is a weighted average of the different μ values instead. Therefore, once the tissues are averaged, the HU number is inconsistent with the tissues included in the voxel and high attenuation structures, like calcium, are over represented (107).

From the clinical standpoint, this is corroborated by a Raff's et al. study (24) demonstrating that a high calcified plaque burden severely affects coronary CTA diagnostic sensitivity and specificity, compared to invasive angiography. Moreover, Leber et al. (91) demonstrated that whereas non-calcified and mixed plaque volumes were systematically underestimated by MDCT compared to IVUS (59.8 ± 76.6 mm^3 vs. 67.7 ± 67.9 mm^3 and 47.7 ± 87.5 mm^3 vs. 57.5 ± 99.4 mm^3, respectively, $p < 0.03$), calcified plaque volumes were overestimated (65.8 ± 110.0 mm^3 vs. 53.2 ± 90.3 mm^3, p = NS).

To improve the diagnostic accuracy of coronary CTA in presence of calcifications we adopted a different setting of window width and window level to analyze this type of plaques and we selected the subgroup of

sections found to have a calcified plaque component at IVUS. Again, coronary CTA systematically overestimated the mean vessel and lumen CSA (18.5 ± 7.1 mm^2 vs. 21.6 ± 7.7 mm^2 and 8.8 ± 4.5 mm^2 vs. 12.4 ± 4.4 mm^2, IVUS and coronary CTA, respectively, $p < 0.01$), and underestimated only slightly the mean plaque area and burden (9.7 ± 3.7 mm^2 vs. 9.2 ± 6.1 mm^2 and 0.5 ± 0.1 vs. 0.4 ± 0.2 mm^2, IVUS and coronary CTA, respectively, $p < 0.01$). Also in this subgroup, coronary CTA proved to predict with good accuracy mean vessel and lumen CSA determined at IVUS (adjusted R^2 of 0.5 ($p < 0.0001$), 0.6 ($p < 0.0001$), respectively), whereas had only low accuracy in predicting the mean plaque area and burden (adjusted R^2 of 0.2 ($p = 0.02$), and 0.2 ($p = 0.04$), respectively).

Therefore, with appropriate reading settings, it's possible to reliably assess with coronary CTA vessel and lumen CSA in presence of atherosclerotic calcified plaques, theoretically preserving the high diagnostic yield in this condition.

Coronary Computed Tomography Angiography Plaque Tissue Characterization

Acute coronary syndromes are precipitated by the development of an intraluminal coronary thrombus, associated with three plaque characteristics: plaque rupture, plaque erosion, and calcified nodules (73). Plaque rupture occurs in a majority of lesions that have overlying thrombi and its histological precursor has been designated as the TCFA, defined as a lesion with a fibrous cap 65 μm thick, infiltrated with macrophages, with a well developed necrotic core (73).

Detecting *in vivo* plaques at risk of rupture would allow a preventive medical or interventional therapeutic action to avoid acute catastrophic

events. Intravascular ultrasound-VH is one of the most promising tools developed with this aim. It uses spectral analysis of IVUS radiofrequency data to construct tissue maps that classify plaques into four major components: a) fibrous, b) fibro-fatty, c) necrotic core, and d) calcium. These components of the atherosclerotic plaque may be visualized on histological sections of coronary arteries stained with Movat pentachrome: a) fibrous plaque comprised of densely packed collagen; b) fibro-fatty plaque consists of collagen and interspersed lipid; c) calcified necrotic plaque that includes cholesterol clefts, foam cells, and micro-calcifications; and d) calcified plaque without adjacent necrosis (66).

In an *ex vivo* experiment, IVUS-VH was able to identify the four plaque types when compared with the corresponding histological sections with a sensitivity, specificity, and predictive accuracy of 80–92% (66). Moreover, IVUS-VH identified plaque components with a good accuracy *in vivo* when compared with histological sections obtained from DCA (67). However, the accuracy of these findings was challenged by a study from Granada et al. (68) in an atherosclerotic porcine model. In fact, when compared with histology, IVUS-VH identified plaque components with a disappointing low accuracy of 38–58%.

Noteworthy, the current literature on the IVUS-VH have significant methodological flaws and therefore more studies are required to validate this technique (69). The construction and validation of tissue maps for IVUS-VH-identified plaque components by Movat pentachrome stain might be not optimal for plaque characterization. Moreover, a histological section and an IVUS-VH image represent different plaque thickness. In fact, a histological section may be as thin as 4 μm, whereas IVUS-VH data derives from an ultrasound beam whose width may be as great as 300 μm.

Finally, the porcine lesions created by liposome injection in the work by Granada et al. (68), do not mimic exactly human atherosclerosis.

Few studies confirm indirectly the validity of IVUS-VH tissue plaque characterization, but conclusion about its reliability warrants results from longitudinal studies (i.e. the ongoing PROSPECT trial). Provided its close association with coronary thrombosis, a surrogate for histological TCFA will be relevant information to define the patient risk of future events. Rodriguez-Granillo et al. (77) performed an analysis to detect TCFA with IVUS-VH in 55 patients and determined that IVUS-derived TCFA was more prevalent in ACS patients. A potential limitation of this study is the axial resolution and spatial accuracy of IVUS-VH. Intravascular ultrasound-VH has an axial resolution of 150 μm and spatial accuracy of 240 μm (66), whereas the accepted histological definition for TCFA requires a thinner fibrous cap (73). Moreover, IVUS-VH cannot visualize cellular components such as T cells and macrophages, both crucial features of histological TCFA.

Another characteristic of vulnerable plaques is the positive remodeling. Therefore, investigators have used IVUS-VH to assess plaque composition in areas of expansive remodeling (78, 79). Lesions with expansive remodeling had a larger necrotic core and less fibrous tissue when compared with non-remodeled lesions or lesions with constrictive remodeling (decrease in the EEM CSA). Lesions with expansive remodeling were predominantly composed of fibro-fatty tissue (fibroatheromatous) or IVUS- derived TCFA. In contrast, only a small number of lesions with constrictive remodeling were fibroatheromatous and none had IVUS-derived TCFA (78). These cross-sectional studies suggest that atherosclerotic lesions with expansive remodeling have different plaque composition than lesions with constrictive remodeling. It

remains unproved whether these compositional differences are predictive of thrombotic events.

Autopsy studies suggest that the majority of occlusive intracoronary thrombotic events arise from plaque rupture. Therefore, assessment of ruptured plaque may provide insight into the features of vulnerable plaque. Rodriguez-Granillo et al. (80) recently described IVUS-VH-derived plaque composition in lesions with plaque rupture. Forty patients with ACS underwent three-vessel IVUS. Plaque rupture occurred in 28 lesions (20 patients). Ruptured lesions compared with lesions without plaque rupture had similar plaque burden but a larger vessel CSA, findings indicative of greater expansive remodeling in ruptured lesions. Ruptured plaques also had a greater percentage of necrotic core. This study is consistent with earlier reports that linked expansive remodeling with coronary events and reveals a correlation between necrotic core and plaque rupture.

To test the hypothesis that non-invasive tissue plaque characterization is possible, we compared the plaque composition derived at IVUS-VH with coronary CTA. Despite overestimating the necrotic core (5.2 ± 3.9 mm^2 vs. 11.9 ± 5.1 mm^2 IVUS and CT, respectively) and the calcified component (2.3 ± 1.7 mm^2 vs. 29.8 ± 14.7 mm^2 IVUS and CT, respectively), coronary CTA proved to predict well the atherosclerotic plaques tissue characteristics compared to IVUS-VH (adjusted R^2 0.8 for necrotic core ($p = 0.02$) and 0.7 for calcified ($p = 0.02$).

Therefore we were able to prove for the first time that coronary CTA could be a valuable tool to non-invasively characterize atherosclerotic plaques.

Limitations of the Study

Ethical reasons drove our decision to select for IVUS imaging only patients with non-obstructive coronary stenosis at invasive coronary angiography. Therefore, our patient cohort is indubitably selected and generalizing our results to severe coronary artery stenoses is not warranted.

A huge effort in multiple research centers is ongoing to *in vivo* characterize atherosclerotic plaques prone to rupture. Accomplishing this in a cross-sectional study requires enrollment of ACS patients, to define the tissue characteristics of the culprit lesion. However, we included in our study only patients with stable angina. In our institutions ACS patients usually undergo an early invasive path, i.e. invasive coronary angiography within the first 24 hours after admission to the hospital (108). Triaging these patients with coronary CTA, which currently has not proved being beneficial in this setting, outside a clinical trial that could demonstrate its efficacy, was thought to be unethical. We would expose these patients to additional 10-14 mSV of radiation (20) and to additional 60-80 ml of iodine contrast, increasing the risk associated to radiation exposure (109) and of renal failure.

However, demonstrating that coronary CTA is able to predict IVUS-VH-derived atherosclerotic plaques features in stable angina patients is an important initial step in trying to determine the suitability of this technique for detection of vulnerable patients. Moreover, including only patients with stable features could represent a plus of the study, because this is the population that would derive more benefits from a non-invasive detection of vulnerable plaque features.

Finally, in our study we correlated coronary CTA to IVUS-VH findings, while is missing a comparison with the histology analysis, the

current gold standard for plaque tissue characterization. In explanted human atherosclerotic arteries (66) and in DCA specimens (67) IVUS-VH-derived plaque composition proved to be in agreement with the corresponding histological sections. Granada et al. (68) recently questioned the accuracy of IVUS-VH, because in an atherosclerotic porcine model it didn't compare favorably with histology. However, the porcine lesions created by liposome injection in this study, do not mimic exactly human atherosclerosis, and this could explain the discrepancy between these studies.

Moreover, despite IVUS-VH possibly lacks accuracy in comparison with histology, a recent study on ACS patients can indirectly corroborate the relevance of *in vivo* plaque tissue characterization. In fact, Rodriguez-Granillo et al. (77) demonstrated that IVUS-VH-derived TCFA was more prevalent in ACS patients compared to chronic angina patients.

Conclusions

Our study demonstrated that coronary CTA is a robust technique in measuring vessel and lumen CSA in presence of calcified and non-calcified atherosclerotic coronary plaques. Despite the measurement accuracy for mean plaque area and burden is moderate-low, "virtual histology" is feasible at coronary CTA and its non-invasive plaque characterization predicts IVUS-VH results. Therefore we were able to prove for the first time that coronary CTA could be a valuable tool to non-invasively characterize atherosclerotic plaques.

Figures

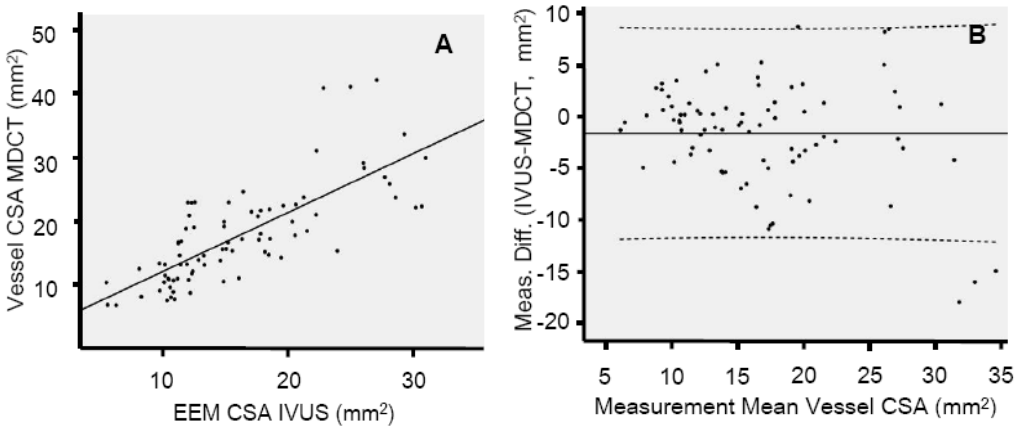

Figure 1. A, Scatterplot of vessel cross-sectional area (CSA) measured at multidetector computed tomography (MDCT) and external elastic membrane (EEM) CSA measured at intravascular ultrasound (IVUS) showed a significant correlation (R^2 0.6, p <0.0001). B, Bland-Altman analysis. Solid line indicates systematic error (mean difference, -1.6 mm^2); hatched lines, limits of agreement.

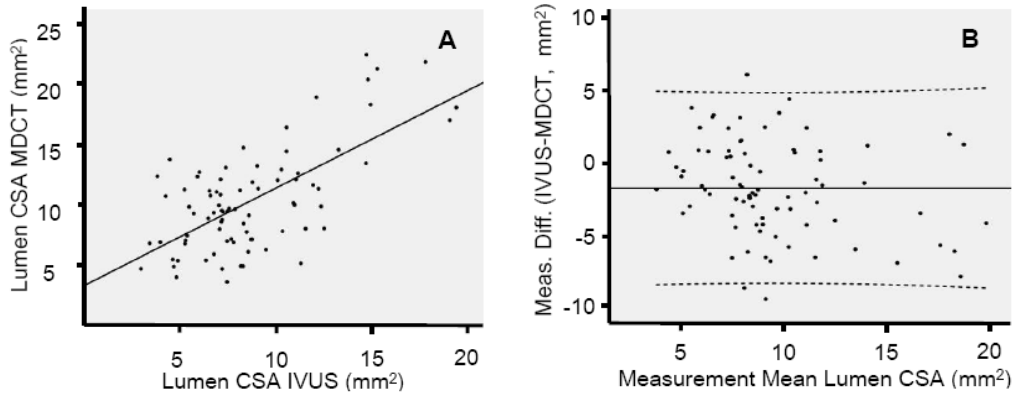

Figure 2. A, Scatterplot of lumen cross-sectional area (CSA) measured at multidetector computed tomography (MDCT) and at intravascular ultrasound (IVUS) showed a significant correlation (R^2 0.5, p <0.0001). B, Bland-Altman analysis. Solid line indicates systematic error (mean difference, -1.8 mm^2); hatched lines, limits of agreement.

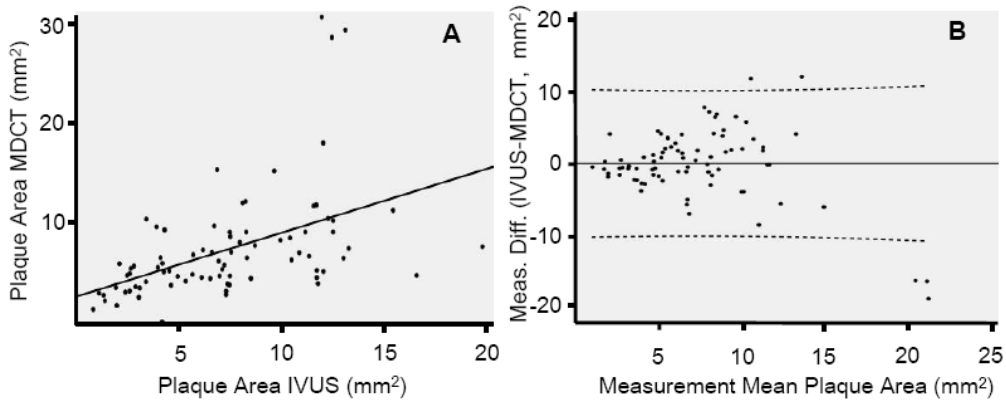

Figure 3. A, Scatterplot of plaque cross-sectional area (CSA) measured at multidetector computed tomography (MDCT) and at intravascular ultrasound (IVUS) showed a significant correlation (R^2 0.3, $p < 0.0001$). B, Bland-Altman analysis. Solid line indicates systematic error (mean difference, 0.1 mm^2); hatched lines, limits of agreement.

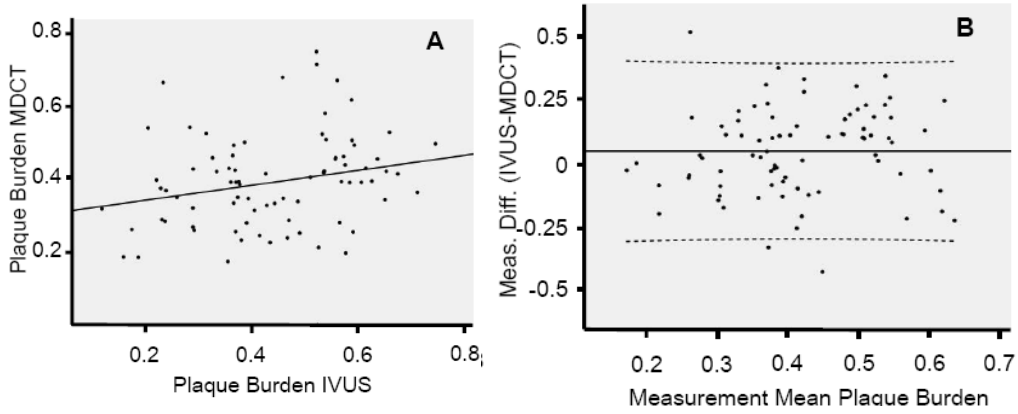

Figure 4. A, Scatterplot of plaque burden measured at multidetector computed tomography (MDCT) and at intravascular ultrasound (IVUS) showed a significant correlation (R^2 0.2, $p = 0.04$). B, Bland-Altman analysis. Solid line indicates systematic error (mean difference, 0.03); hatched lines, limits of agreement.

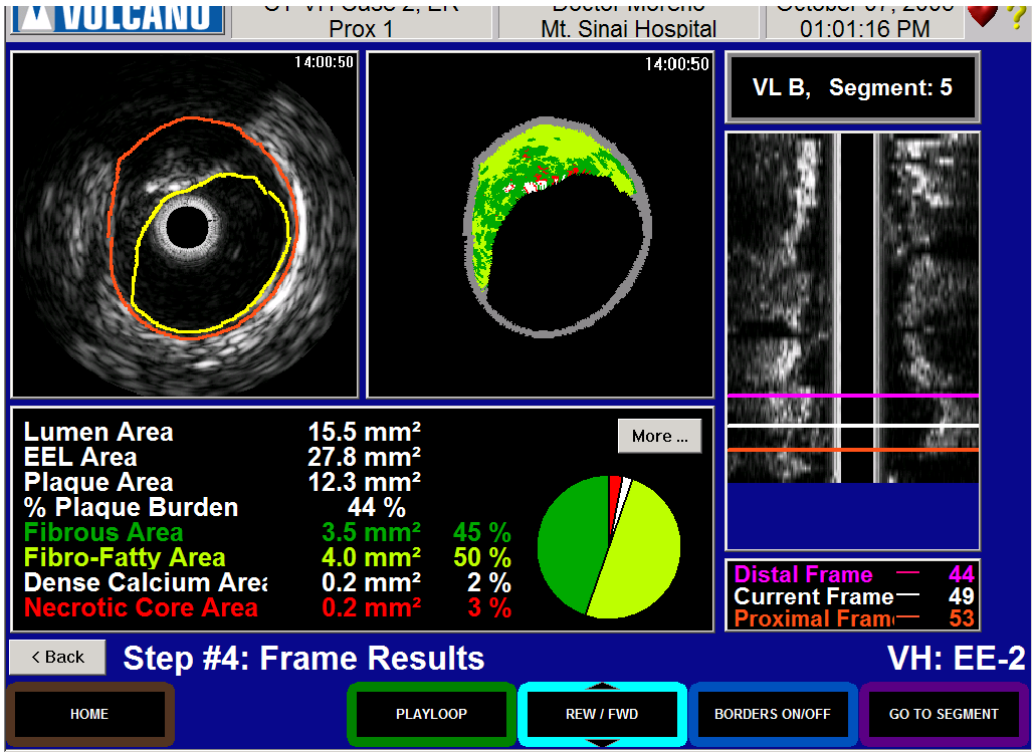

Figure 5. Example of Intravascular Ultrasound-Virtual Histology (IVUS-VH) software output. [Volcano Corporation, Rancho Cordova, CA, USA]. Atherosclerotic plaque components at IVUS-VH: a) fibrous [labeled green], b) fibro-fatty [labeled greenish-yellow], c) necrotic core [labeled red], and d) calcium [labeled white].

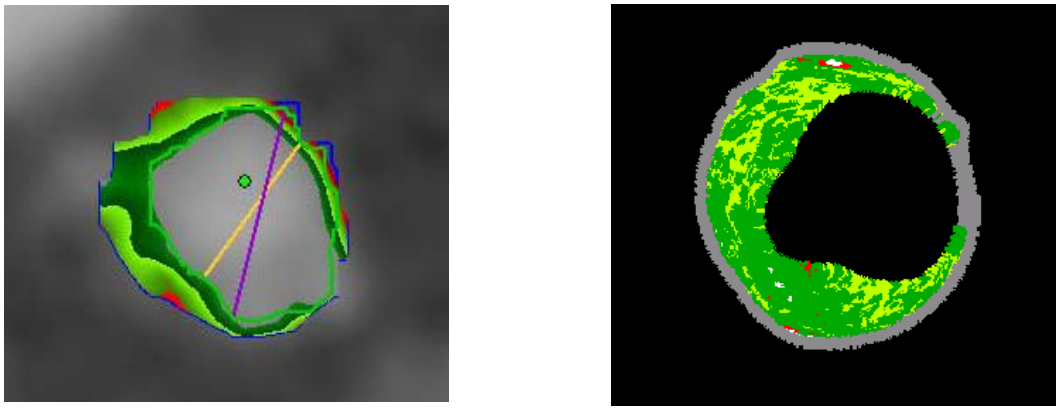

Figure 6. Representative example of atherosclerotic non-calcified plaque at coronary computed tomography angiography (left) and intravascular ultrasound-virtual histology (right) (Atherosclerotic plaque components are: a) fibrous [labeled green], b) fibro-fatty [labeled greenish-yellow], c) necrotic core [labeled red], and d) calcium [labeled white]).

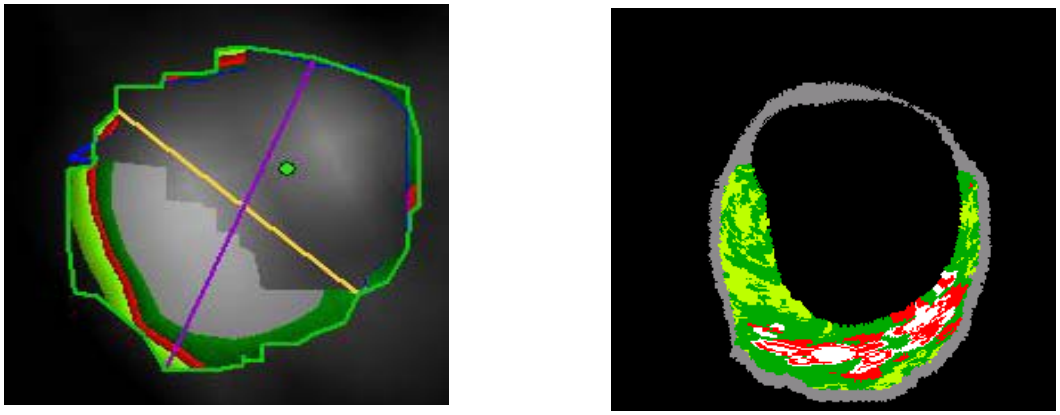

Figure 7. Representative example of atherosclerotic calcified plaque with a necrotic core component at coronary computed tomography angiography (left) and intravascular ultrasound-virtual histology (right).

References

1. Noto TJ, Jr., Johnson LW, Krone R, et al. Cardiac catheterization 1990: a report of the Registry of the Society for Cardiac Angiography and Interventions (SCA&I). Cathet Cardiovasc Diagn 1991; 24:75-83.
2. Johnson LW, Lozner EC, Johnson S, et al. Coronary arteriography 1984-1987: a report of the Registry of the Society for Cardiac Angiography and Interventions. I. Results and complications. Cathet Cardiovasc Diagn 1989; 17:5-10.
3. Johnson LW, Krone R. Cardiac catheterization 1991: a report of the Registry of the Society for Cardiac Angiography and Interventions (SCA&I). Cathet Cardiovasc Diagn 1993; 28:219-20.
4. Bashore TM, Bates ER, Berger PB, et al. American College of Cardiology/Society for Cardiac Angiography and Interventions Clinical Expert Consensus Document on cardiac catheterization laboratory standards. A report of the American College of Cardiology Task Force on Clinical Expert Consensus Documents. J Am Coll Cardiol 2001; 37:2170-214.
5. Achenbach S, Werner GD. Computed tomography of the heart. In: Zipes DP, Libby P, Bonow RO, Braunwald E, editors. Braunwald's Heart Disease. Elsevier Saunders, 2005:355-71.
6. Poon M. Technology insight: Cardiac CT angiography. Nat Clin Pract Cardiovasc Med 2006; 3:265-75.
7. Budoff MJ, Poon M, Maiolino G. Computed tomography of the heart. In: Fuster V, O'Rourke RA, Walsh RA, Poole-Wilson PA, editors. Hurst's. The Heart. McGraw Hill Corporation, 2008:577-606.
8. Schroeder S, Kopp AF, Kuettner A, et al. Influence of heart rate on vessel visibility in noninvasive coronary angiography using new

multislice computed tomography: experience in 94 patients. Clin Imaging 2002; 26:106-11.

9. Nieman K, Rensing BJ, van Geuns RJ, et al. Non-invasive coronary angiography with multislice spiral computed tomography: impact of heart rate. Heart 2002; 88:470-4.
10. Hong C, Becker CR, Huber A, et al. ECG-gated reconstructed multi-detector row CT coronary angiography: effect of varying trigger delay on image quality. Radiology 2001; 220:712-7.
11. Leschka S, Wildermuth S, Boehm T, et al. Noninvasive coronary angiography with 64-section CT: effect of average heart rate and heart rate variability on image quality. Radiology 2006; 241:378-85.
12. Achenbach S, Ropers D, Holle J, Muschiol G, Daniel WG, Moshage W. In-plane coronary arterial motion velocity: measurement with electron-beam CT. Radiology 2000; 216:457-63.
13. Lu B, Mao SS, Zhuang N, et al. Coronary artery motion during the cardiac cycle and optimal ECG triggering for coronary artery imaging. Invest Radiol 2001; 36:250-6.
14. Scanlon PJ, Faxon DP, Audet AM, et al. ACC/AHA guidelines for coronary angiography. A report of the American College of Cardiology/American Heart Association Task Force on practice guidelines (Committee on Coronary Angiography). Developed in collaboration with the Society for Cardiac Angiography and Interventions. J Am Coll Cardiol 1999; 33:1756-824.
15. Nissen SE, Yock P. Intravascular ultrasound: novel pathophysiological insights and current clinical applications. Circulation 2001; 103:604-16.

16. Cademartiri F, Schuijf JD, Mollet NR, et al. Multislice CT coronary angiography: how to do it and what is the current clinical performance? Eur J Nucl Med Mol Imaging 2005; 32:1337-47.
17. Scheffel H, Alkadhi H, Plass A, et al. Accuracy of dual-source CT coronary angiography: First experience in a high pre-test probability population without heart rate control. Eur Radiol 2006; 16:2739-47.
18. Hendel RC, Patel MR, Kramer CM, et al. ACCF/ACR/SCCT/SCMR/ ASNC/NASCI/SCAI/SIR 2006 appropriateness criteria for cardiac computed tomography and cardiac magnetic resonance imaging: a report of the American College of Cardiology Foundation Quality Strategic Directions Committee Appropriateness Criteria Working Group, American College of Radiology, Society of Cardiovascular Computed Tomography, Society for Cardiovascular Magnetic Resonance, American Society of Nuclear Cardiology, North American Society for Cardiac Imaging, Society for Cardiovascular Angiography and Interventions, and Society of Interventional Radiology. J Am Coll Cardiol 2006; 48:1475-97.
19. Leschka S, Alkadhi H, Plass A, et al. Accuracy of MSCT coronary angiography with 64-slice technology: first experience. Eur Heart J 2005; 26:1482-7.
20. Leber AW, Knez A, von ZF, et al. Quantification of obstructive and nonobstructive coronary lesions by 64-slice computed tomography: a comparative study with quantitative coronary angiography and intravascular ultrasound. J Am Coll Cardiol 2005; 46:147-54.
21. Ropers D, Rixe J, Anders K, et al. Usefulness of multidetector row spiral computed tomography with 64- x 0.6-mm collimation and 330-

ms rotation for the noninvasive detection of significant coronary artery stenoses. Am J Cardiol 2006; 97:343-8.

22. Fine JJ, Hopkins CB, Ruff N, Newton FC. Comparison of accuracy of 64-slice cardiovascular computed tomography with coronary angiography in patients with suspected coronary artery disease. Am J Cardiol 2006; 97:173-4.
23. Mollet NR, Cademartiri F, van Mieghem CA, et al. High-resolution spiral computed tomography coronary angiography in patients referred for diagnostic conventional coronary angiography. Circulation 2005; 112:2318-23.
24. Raff GL, Gallagher MJ, O'Neill WW, Goldstein JA. Diagnostic accuracy of noninvasive coronary angiography using 64-slice spiral computed tomography. J Am Coll Cardiol 2005; 46:552-7.
25. Nikolaou K, Knez A, Rist C, et al. Accuracy of 64-MDCT in the diagnosis of ischemic heart disease. AJR Am J Roentgenol 2006; 187:111-7.
26. Schlosser T, Mohrs OK, Magedanz A, et al. Noninvasive coronary angiography using 64-detector-row computed tomography in patients with a low to moderate pretest probability of significant coronary artery disease. Acta Radiol 2007; 48:300-7.
27. Muhlenbruch G, Seyfarth T, Soo CS, Pregalathan N, Mahnken AH. Diagnostic value of 64-slice multi-detector row cardiac CTA in symptomatic patients. Eur Radiol 2007; 17:603-9.
28. Meijboom WB, Mollet NR, van Mieghem CA, et al. 64-Slice CT coronary angiography in patients with non-ST elevation acute coronary syndrome. Heart 2007; 93:1386-92.

29. Schuijf JD, Pundziute G, Jukema JW, et al. Diagnostic accuracy of 64-slice multislice computed tomography in the noninvasive evaluation of significant coronary artery disease. Am J Cardiol 2006; 98:145-8.
30. Oncel D, Oncel G, Tastan A, Tamci B. Detection of significant coronary artery stenosis with 64-section MDCT angiography. Eur J Radiol 2007; 62:394-405.
31. Cademartiri F, Maffei E, Palumbo A, et al. Diagnostic accuracy of 64-slice computed tomography coronary angiography in patients with low-to-intermediate risk. Radiol Med (Torino) 2007; 112:969-81.
32. Herzog C, Zwerner PL, Doll JR, et al. Significant coronary artery stenosis: comparison on per-patient and per-vessel or per-segment basis at 64-section CT angiography. Radiology 2007; 244:112-20.
33. Johnson TR, Nikolaou K, Busch S, et al. Diagnostic accuracy of dual-source computed tomography in the diagnosis of coronary artery disease. Invest Radiol 2007; 42:684-91.
34. Leber AW, Johnson T, Becker A, et al. Diagnostic accuracy of dual-source multi-slice CT-coronary angiography in patients with an intermediate pretest likelihood for coronary artery disease. Eur Heart J 2007; 28:2354-60.
35. Malagutti P, Nieman K, Meijboom WB, et al. Use of 64-slice CT in symptomatic patients after coronary bypass surgery: evaluation of grafts and coronary arteries. Eur Heart J 2007; 28:1879-85.
36. Ropers D, Pohle FK, Kuettner A, et al. Diagnostic accuracy of noninvasive coronary angiography in patients after bypass surgery using 64-slice spiral computed tomography with 330-ms gantry rotation. Circulation 2006; 114:2334-41.

37. Pache G, Saueressig U, Frydrychowicz A, et al. Initial experience with 64-slice cardiac CT: non-invasive visualization of coronary artery bypass grafts. Eur Heart J 2006; 27:976-80.
38. Onuma Y, Tanabe K, Chihara R, et al. Evaluation of coronary artery bypass grafts and native coronary arteries using 64-slice multidetector computed tomography. Am Heart J 2007; 154:519-26.
39. Meyer TS, Martinoff S, Hadamitzky M, et al. Improved noninvasive assessment of coronary artery bypass grafts with 64-slice computed tomographic angiography in an unselected patient population. J Am Coll Cardiol 2007; 49:946-50.
40. Gilard M, Cornily JC, Pennec PY, et al. Assessment of coronary artery stents by 16 slice computed tomography. Heart 2006; 92:58-61.
41. Rixe J, Achenbach S, Ropers D, et al. Assessment of coronary artery stent restenosis by 64-slice multi-detector computed tomography. Eur Heart J 2006; 27:2567-72.
42. Cademartiri F, Schuijf JD, Pugliese F, et al. Usefulness of 64-slice multislice computed tomography coronary angiography to assess in-stent restenosis. J Am Coll Cardiol 2007; 49:2204-10.
43. Isner JM, Kishel J, Kent KM, Ronan JA, Jr., Ross AM, Roberts WC. Accuracy of angiographic determination of left main coronary arterial narrowing. Angiographic--histologic correlative analysis in 28 patients. Circulation 1981; 63:1056-64.
44. Vlodaver Z, Frech R, Van Tassel RA, Edwards JE. Correlation of the antemortem coronary arteriogram and the postmortem specimen. Circulation 1973; 47:162-9.

45. Zir LM, Miller SW, Dinsmore RE, Gilbert JP, Harthorne JW. Interobserver variability in coronary angiography. Circulation 1976; 53:627-32.
46. Galbraith JE, Murphy ML, de SN. Coronary angiogram interpretation. Interobserver variability. JAMA 1978; 240:2053-6.
47. Roberts WC, Jones AA. Quantitation of coronary arterial narrowing at necropsy in sudden coronary death: analysis of 31 patients and comparison with 25 control subjects. Am J Cardiol 1979; 44:39-45.
48. Topol EJ, Nissen SE. Our preoccupation with coronary luminology. The dissociation between clinical and angiographic findings in ischemic heart disease. Circulation 1995; 92:2333-42.
49. Glagov S, Weisenberg E, Zarins CK, Stankunavicius R, Kolettis GJ. Compensatory enlargement of human atherosclerotic coronary arteries. N Engl J Med 1987; 316:1371-5.
50. Tobis JM, Mallery J, Mahon D, et al. Intravascular ultrasound imaging of human coronary arteries in vivo. Analysis of tissue characterizations with comparison to in vitro histological specimens. Circulation 1991; 83:913-26.
51. Hodgson JM, Reddy KG, Suneja R, Nair RN, Lesnefsky EJ, Sheehan HM. Intracoronary ultrasound imaging: correlation of plaque morphology with angiography, clinical syndrome and procedural results in patients undergoing coronary angioplasty. J Am Coll Cardiol 1993; 21:35-44.
52. Fisher LD, Judkins MP, Lesperance J, et al. Reproducibility of coronary arteriographic reading in the coronary artery surgery study (CASS). Cathet Cardiovasc Diagn 1982; 8:565-75.

53. Keren G, Leon MB. Characterization of atherosclerotic lesions by intravascular ultrasound: possible role in unstable coronary syndromes and in interventional therapeutic procedures. Am J Cardiol 1991; 68:85B-91B.
54. Mintz GS, Douek P, Pichard AD, et al. Target lesion calcification in coronary artery disease: an intravascular ultrasound study. J Am Coll Cardiol 1992; 20:1149-55.
55. Mintz GS, Painter JA, Pichard AD, et al. Atherosclerosis in angiographically "normal" coronary artery reference segments: an intravascular ultrasound study with clinical correlations. J Am Coll Cardiol 1995; 25:1479-85.
56. Mintz GS, Nissen SE, Anderson WD, et al. American College of Cardiology Clinical Expert Consensus Document on Standards for Acquisition, Measurement and Reporting of Intravascular Ultrasound Studies (IVUS). A report of the American College of Cardiology Task Force on Clinical Expert Consensus Documents. J Am Coll Cardiol 2001; 37:1478-92.
57. Nissen SE, Grines CL, Gurley JC, et al. Application of a new phased-array ultrasound imaging catheter in the assessment of vascular dimensions. In vivo comparison to cineangiography. Circulation 1990; 81:660-6.
58. Nissen SE, Gurley JC, Grines CL, et al. Intravascular ultrasound assessment of lumen size and wall morphology in normal subjects and patients with coronary artery disease. Circulation 1991; 84:1087-99.

59. Tobis JM, Mallery JA, Gessert J, et al. Intravascular ultrasound cross-sectional arterial imaging before and after balloon angioplasty in vitro. Circulation 1989; 80:873-82.
60. Schaar JA, van der Steen AF, Mastik F, Baldewsing RA, Serruys PW. Intravascular palpography for vulnerable plaque assessment. J Am Coll Cardiol 2006; 47:C86-C91.
61. Nishimura RA, Edwards WD, Warnes CA, et al. Intravascular ultrasound imaging: in vitro validation and pathologic correlation. J Am Coll Cardiol 1990; 16:145-54.
62. Zhang X, McKay CR, Sonka M. Tissue characterization in intravascular ultrasound images. IEEE Trans Med Imaging 1998; 17:889-99.
63. Gussenhoven EJ, Essed CE, Lancee CT, et al. Arterial wall characteristics determined by intravascular ultrasound imaging: an in vitro study. J Am Coll Cardiol 1989; 14:947-52.
64. Di MC, The SH, Madretsma S, et al. Detection and characterization of vascular lesions by intravascular ultrasound: an in vitro study correlated with histology. J Am Soc Echocardiogr 1992; 5:135-46.
65. Sipahi I, Nicholls SJ, Tuzcu EM. Recent trends in coronary intravascular ultrasound: tracking atherosclerosis, pursuit of vulnerable plaques, and beyond. J Nucl Cardiol 2006; 13:91-6.
66. Nair A, Kuban BD, Tuzcu EM, Schoenhagen P, Nissen SE, Vince DG. Coronary plaque classification with intravascular ultrasound radiofrequency data analysis. Circulation 2002; 106:2200-6.
67. Nasu K, Tsuchikane E, Katoh O, et al. Accuracy of in vivo coronary plaque morphology assessment: a validation study of in vivo virtual

histology compared with in vitro histopathology. J Am Coll Cardiol 2006; 47:2405-12.

68. Granada JF, Wallace-Bradley D, Win HK, et al. In vivo plaque characterization using intravascular ultrasound-virtual histology in a porcine model of complex coronary lesions. Arterioscler Thromb Vasc Biol 2007; 27:387-93.
69. Mehta SK, McCrary JR, Frutkin AD, Dolla WJ, Marso SP. Intravascular ultrasound radiofrequency analysis of coronary atherosclerosis: an emerging technology for the assessment of vulnerable plaque. Eur Heart J 2007; 28:1283-8.
70. Burke AP, Joner M, Virmani R. IVUS-VH: a predictor of plaque morphology? Eur Heart J 2006; 27:1889-90.
71. Burke AP, Farb A, Malcom GT, Liang YH, Smialek J, Virmani R. Coronary risk factors and plaque morphology in men with coronary disease who died suddenly. N Engl J Med 1997; 336:1276-82.
72. Burke AP, Farb A, Malcom GT, Liang Y, Smialek J, Virmani R. Effect of risk factors on the mechanism of acute thrombosis and sudden coronary death in women. Circulation 1998; 97:2110-6.
73. Virmani R, Kolodgie FD, Burke AP, Farb A, Schwartz SM. Lessons from sudden coronary death: a comprehensive morphological classification scheme for atherosclerotic lesions. Arterioscler Thromb Vasc Biol 2000; 20:1262-75.
74. Schoenhagen P, Ziada KM, Kapadia SR, Crowe TD, Nissen SE, Tuzcu EM. Extent and direction of arterial remodeling in stable versus unstable coronary syndromes : an intravascular ultrasound study. Circulation 2000; 101:598-603.

75. Varnava AM, Mills PG, Davies MJ. Relationship between coronary artery remodeling and plaque vulnerability. Circulation 2002; 105:939-43.
76. Ehara S, Kobayashi Y, Yoshiyama M, et al. Spotty calcification typifies the culprit plaque in patients with acute myocardial infarction: an intravascular ultrasound study. Circulation 2004; 110:3424-9.
77. Rodriguez-Granillo GA, Garcia-Garcia HM, Mc Fadden EP, et al. In vivo intravascular ultrasound-derived thin-cap fibroatheroma detection using ultrasound radiofrequency data analysis. J Am Coll Cardiol 2005; 46:2038-42.
78. Rodriguez-Granillo GA, Serruys PW, Garcia-Garcia HM, et al. Coronary artery remodelling is related to plaque composition. Heart 2006; 92:388-91.
79. Fujii K, Carlier SG, Mintz GS, et al. Association of plaque characterization by intravascular ultrasound virtual histology and arterial remodeling. Am J Cardiol 2005; 96:1476-83.
80. Rodriguez-Granillo GA, Garcia-Garcia HM, Valgimigli M, et al. Global characterization of coronary plaque rupture phenotype using three-vessel intravascular ultrasound radiofrequency data analysis. Eur Heart J 2006; 27:1921-7.
81. Motoyama S, Kondo T, Sarai M, et al. Multislice computed tomographic characteristics of coronary lesions in acute coronary syndromes. J Am Coll Cardiol 2007; 50:319-26.
82. Rioufol G, Finet G, Ginon I, et al. Multiple atherosclerotic plaque rupture in acute coronary syndrome: a three-vessel intravascular ultrasound study. Circulation 2002; 106:804-8.

83. Spagnoli LG, Bonanno E, Mauriello A, et al. Multicentric inflammation in epicardial coronary arteries of patients dying of acute myocardial infarction. J Am Coll Cardiol 2002; 40:1579-88.
84. Caussin C, Larchez C, Ghostine S, et al. Comparison of coronary minimal lumen area quantification by sixty-four-slice computed tomography versus intravascular ultrasound for intermediate stenosis. Am J Cardiol 2006; 98:871-6.
85. Dragu R, Kerner A, Gruberg L, et al. Angiographically uncertain left main coronary artery narrowings: correlation with multidetector computed tomography and intravascular ultrasound. Int J Cardiovasc Imaging 2007.
86. Moselewski F, Ropers D, Pohle K, et al. Comparison of measurement of cross-sectional coronary atherosclerotic plaque and vessel areas by 16-slice multidetector computed tomography versus intravascular ultrasound. Am J Cardiol 2004; 94:1294-7.
87. van Mieghem CA, McFadden EP, de Feyter PJ, et al. Noninvasive detection of subclinical coronary atherosclerosis coupled with assessment of changes in plaque characteristics using novel invasive imaging modalities: the Integrated Biomarker and Imaging Study (IBIS). J Am Coll Cardiol 2006; 47:1134-42.
88. Iriart X, Brunot S, Coste P, et al. Early characterization of atherosclerotic coronary plaques with multidetector computed tomography in patients with acute coronary syndrome: a comparative study with intravascular ultrasound. Eur Radiol 2007; 17:2581-8.
89. Achenbach S, Moselewski F, Ropers D, et al. Detection of calcified and noncalcified coronary atherosclerotic plaque by contrast-

enhanced, submillimeter multidetector spiral computed tomography: a segment-based comparison with intravascular ultrasound. Circulation 2004; 109:14-7.

90. Leber AW, Knez A, Becker A, et al. Accuracy of multidetector spiral computed tomography in identifying and differentiating the composition of coronary atherosclerotic plaques: a comparative study with intracoronary ultrasound. J Am Coll Cardiol 2004; 43:1241-7.
91. Leber AW, Becker A, Knez A, et al. Accuracy of 64-slice computed tomography to classify and quantify plaque volumes in the proximal coronary system: a comparative study using intravascular ultrasound. J Am Coll Cardiol 2006; 47:672-7.
92. Schroeder S, Kopp AF, Baumbach A, et al. Noninvasive detection and evaluation of atherosclerotic coronary plaques with multislice computed tomography. J Am Coll Cardiol 2001; 37:1430-5.
93. Kopp AF, Schroeder S, Baumbach A, et al. Non-invasive characterisation of coronary lesion morphology and composition by multislice CT: first results in comparison with intracoronary ultrasound. Eur Radiol 2001; 11:1607-11.
94. Schroeder S, Kuettner A, Leitritz M, et al. Reliability of differentiating human coronary plaque morphology using contrast-enhanced multislice spiral computed tomography: a comparison with histology. J Comput Assist Tomogr 2004; 28:449-54.
95. Schoenhagen P, Tuzcu EM, Stillman AE, et al. Non-invasive assessment of plaque morphology and remodeling in mildly stenotic coronary segments: comparison of 16-slice computed tomography and intravascular ultrasound. Coron Artery Dis 2003; 14:459-62.

96. Komatsu S, Hirayama A, Omori Y, et al. Detection of coronary plaque by computed tomography with a novel plaque analysis system, 'Plaque Map', and comparison with intravascular ultrasound and angioscopy. Circ J 2005; 69:72-7.
97. Pohle K, Achenbach S, Macneill B, et al. Characterization of non-calcified coronary atherosclerotic plaque by multi-detector row CT: comparison to IVUS. Atherosclerosis 2007; 190:174-80.
98. Pasterkamp G, Schoneveld AH, van der Wal AC, et al. Relation of arterial geometry to luminal narrowing and histologic markers for plaque vulnerability: the remodeling paradox. J Am Coll Cardiol 1998; 32:655-62.
99. Achenbach S, Ropers D, Hoffmann U, et al. Assessment of coronary remodeling in stenotic and nonstenotic coronary atherosclerotic lesions by multidetector spiral computed tomography. J Am Coll Cardiol 2004; 43:842-7.
100. Kitagawa T, Yamamoto H, Ohhashi N, et al. Comprehensive evaluation of noncalcified coronary plaque characteristics detected using 64-slice computed tomography in patients with proven or suspected coronary artery disease. Am Heart J 2007; 154:1191-8.
101. Caussin C, Ohanessian A, Ghostine S, et al. Characterization of vulnerable nonstenotic plaque with 16-slice computed tomography compared with intravascular ultrasound. Am J Cardiol 2004; 94:99-104.
102. Leber AW, Knez A, Becker C, et al. Non-invasive intravenous coronary angiography using electron beam tomography and multislice computed tomography. Heart 2003; 89:633-9.

103. Becker CR, Nikolaou K, Muders M, et al. Ex vivo coronary atherosclerotic plaque characterization with multi-detector-row CT. Eur Radiol 2003; 13:2094-8.
104. Nikolaou K, Becker CR, Muders M, et al. Multidetector-row computed tomography and magnetic resonance imaging of atherosclerotic lesions in human ex vivo coronary arteries. Atherosclerosis 2004; 174:243-52.
105. Austen WG, Edwards JE, Frye RL, et al. A reporting system on patients evaluated for coronary artery disease. Report of the Ad Hoc Committee for Grading of Coronary Artery Disease, Council on Cardiovascular Surgery, American Heart Association. Circulation 1975; 51:5-40.
106. Funabashi N, Kobayashi Y, Kudo M, et al. New method of measuring coronary diameter by electron-beam computed tomographic angiography using adjusted thresholds determined by calibration with aortic opacity. Circ J 2004; 68:769-77.
107. Nakanishi T, Kayashima Y, Inoue R, Sumii K, Gomyo Y. Pitfalls in 16-detector row CT of the coronary arteries. Radiographics 2005; 25:425-38.
108. Anderson JL, Adams CD, Antman EM, et al. ACC/AHA 2007 guidelines for the management of patients with unstable angina/non-ST-Elevation myocardial infarction: a report of the American College of Cardiology/American Heart Association Task Force on Practice Guidelines (Writing Committee to Revise the 2002 Guidelines for the Management of Patients With Unstable Angina/Non-ST-Elevation Myocardial Infarction) developed in collaboration with the American College of Emergency Physicians,

the Society for Cardiovascular Angiography and Interventions, and the Society of Thoracic Surgeons endorsed by the American Association of Cardiovascular and Pulmonary Rehabilitation and the Society for Academic Emergency Medicine. J Am Coll Cardiol 2007; 50:e1-e157.

109. Einstein AJ, Henzlova MJ, Rajagopalan S. Estimating risk of cancer associated with radiation exposure from 64-slice computed tomography coronary angiography. JAMA 2007; 298:317-23.